Dosimetric accuracy of dynamic couch rotation during volumetric modulated arc therapy (DCR-VMAT) for primary brain tumours

Gregory Smyth[1], Philip M Evans[2,3], Jeffrey C Bamber[1], Henry C Mandeville[4], A Rollo Moore[1], Liam C Welsh[4], Frank H Saran[4] and James L Bedford[1]

[1] Joint Department of Physics at The Institute of Cancer Research and The Royal Marsden NHS Foundation Trust, London, United Kingdom
[2] Centre for Vision, Speech and Signal Processing, University of Surrey, Guildford, United Kingdom
[3] National Physical Laboratory, Hampton Road, Teddington, Middlesex, United Kingdom
[4] The Royal Marsden NHS Foundation Trust, Sutton, London, United Kingdom

E-mail: greg.smyth@icr.ac.uk

Submitted 23rd November 2018
Revised 21st February 2019

Abstract. Radiotherapy treatment plans using dynamic couch rotation during volumetric modulated arc therapy (DCR-VMAT) reduce the dose to organs at risk (OARs) compared to coplanar VMAT, while maintaining the dose to the planning target volume (PTV). This paper seeks to validate this finding with measurements. DCR-VMAT treatment plans were produced for five patients with primary brain tumours and delivered using a commercial linear accelerator (linac). Dosimetric accuracy was assessed using point dose and radiochromic film measurements. Linac-recorded mechanical errors were assessed by extracting deviations from log files for multi-leaf collimator (MLC), couch, and gantry positions every 20 ms. Dose distributions, reconstructed from every fifth log file sample, were calculated and used to determine deviations from the treatment plans. Median (range) treatment delivery times were 125 s (123–133 s) for DCR-VMAT, compared to 78 s (64–130 s) for coplanar VMAT. Absolute point doses were 0.8% (0.6–1.7%) higher than prediction. For coronal and sagittal films, respectively, 99.2% (96.7–100%) and 98.1% (92.9–99.0%) of pixels above a 20% low dose threshold reported gamma <1 for 3% and 3 mm criteria. Log file analysis showed similar gantry rotation root-mean-square error (RMSE) for VMAT and DCR-VMAT. Couch rotation RMSE for DCR-VMAT was 0.091° (0.086–0.102°). For delivered dose reconstructions, 100% of pixels above a 5% low dose threshold reported gamma <1 for 2% and 2 mm criteria in all cases. DCR-VMAT, for the primary brain tumour cases studied, can be delivered accurately using a commercial linac.

Keywords: VMAT, Non-coplanar, Trajectory, Verification, Log file, Dose reconstruction

1. Introduction

Radiotherapy treatment plans that use dynamic couch rotation during volumetric modulated arc therapy (DCR-VMAT) improve organ at risk (OAR) sparing over coplanar VMAT, while maintaining planning target volume (PTV) dose coverage (Podgorsak *et al* 1988, Krayenbuehl *et al* 2006, Shaitelman *et al* 2011, Yang *et al* 2011, Popescu *et al* 2013, Smyth *et al* 2013, Fahimian *et al* 2013, MacDonald and Thomas 2015, Wild *et al* 2015, Papp *et al* 2015, Liang *et al* 2015, Smyth *et al* 2016, Wilson *et al* 2017, Langhans *et al* 2018, Lyu *et al* 2018, Dong *et al* 2018, Fix *et al* 2018, Smyth *et al* 2019). Single-arc DCR-VMAT using optimized trajectories has been shown to reduce the contralateral hippocampus, temporal lobe, and cochlea mean dose by 30%, 29%, and 14%, respectively, for a cohort of fifteen primary brain tumour cases (Smyth *et al* 2016). However, to fully realize this modelled OAR sparing, DCR-VMAT plans must be delivered accurately. The International Commission on Radiation Units and Measurements (ICRU) recommends that 85% of measurement points should be within 5% or 5 mm of the planned dose (ICRU 2010), although stricter criteria of 3% and 3 mm are generally used in practice (Clark *et al* 2014). If delivered doses are significantly different from prediction, this could increase the risk of side effects or compromise tumour control. In addition, clinical adoption of DCR-VMAT would be limited if its delivery is significantly slower than coplanar VMAT and requires patient treatment appointments to be extended beyond their current duration.

Dosimetric accuracy and mechanical errors have been reported for some dynamic couch rotation techniques. Fahimian *et al* (2013) and Liang *et al* (2015) investigate the dosimetric accuracy of trajectory modulated arc therapy (TMAT), a combination of dynamic couch rotation and fixed gantry rotation, for two accelerated partial breast irradiation (APBI) cases. Manser *et al* (2018) and Fix *et al* (2018) report the dosimetric accuracy of DCR-VMAT for a prostate case using a manually defined trajectory and a head and neck case using a geometrically optimized trajectory, respectively. As well as dosimetric accuracy, Wilson *et al* (2017) quantify linac-reported mechanical errors during delivery for their mathematically-defined trajectory-based VMAT (TVMAT) technique for four intracranial stereotactic plans from linac log files. Log files record the machine parameters regularly during beam delivery, with the period between log samples depending on the combination of linac manufacturer and control system version (Pasler *et al* 2015).

This paper focuses on investigating the dosimetric accuracy of single-arc DCR-VMAT plans for five primary brain tumour cases. The dosimetric effect of mechanical errors and the static approximation of dynamic couch rotation used during treatment plan dose calculation are investigated for the first time by reconstructing delivered dose distributions from log files. Finally, results are benchmarked against the corresponding coplanar VMAT plans for each of the five cases studied.

Table 1. Diagnosis and planning target volume (PTV) details for all patient cases.

Case	Diagnosis	PTV volume (cm^3)
1	Craniopharyngioma	5.5
2	Craniopharyngioma	31.7
3	Oligoastrocytoma	554.2
4	Astrocytoma	505.6
5	Astrocytoma	151.2

2. Materials and methods

2.1. Beam modelling

A TrueBeam (Varian Medical Systems, Sunnyvale, CA) linac was modelled in the Pinnacle^3 (v9.10, Philips Medical, Madison, WI) and in-house AutoBeam (Bedford 2009, 2013) treatment planning systems (TPS). TrueBeam is the only currently available machine capable of delivering dynamic couch rotation treatment plans, however in principle DCR-VMAT can be delivered on any VMAT capable C-arm linac.

Modelling was performed for a 6 MV beam within Pinnacle^3 using its auto-modelling features and the literature (Chang *et al* 2012, Glide-Hurst *et al* 2013, Philips Medical 2013) to inform modelling parameters. Validation was performed using a 30 cm x 30 cm x 30 cm water phantom with dose calculated on a 2.0 mm x 2.0 mm x 2.0 mm grid. Absolute point doses, relative output factors, percentage depth doses, and relative dose profiles were compared with validation measurements for jaw-defined field sizes. Validation of modulated deliveries was performed by measuring the dosimetric accuracy of coplanar VMAT plans for each patient case.

2.2. Treatment planning and delivery

VMAT and DCR-VMAT plans, each using a single arc, were produced for five patient cases with primary brain tumours (Table 1). Treatment plans for the TrueBeam model were optimized in AutoBeam (v5.5a) to receive 54 Gy in 30 fractions using the objectives described in Table 2. During treatment plan optimization, jaws under the multi-leaf collimator (MLC) banks were set as static and retracted to 10 cm in preparation for TrueBeam delivery. Plans were exported to Pinnacle^3 for final dose calculation using the local clinical standard settings of a 2.5 mm x 2.5 mm x 2.5 mm dose grid resolution and the Adaptive Convolve algorithm. Dose calculation for DCR-VMAT was performed using multiple static control points, each with associated gantry and couch positions, as is standard for coplanar VMAT within Pinnacle^3.

For DCR-VMAT plans, patient-specific trajectories were determined using the geometric heuristic optimization technique described previously (Smyth *et al* 2013, 2016). The organs at risk and their relative importance values used during treatment plan optimization were also used for trajectory optimization (Table 2). Each DCR-

Table 2. Optimization parameters used within AutoBeam for VMAT and DCR-VMAT treatment planning. Organs at risk and their relative importance values were also used for DCR-VMAT trajectory optimization. RMS = root mean square deviation.

Region of interest	Objective	Relative importance
PTV	Minimize RMS around 54 Gy	100
Brainstem	Minimize maximum dose	10
Globes	Minimize maximum dose	5
Optic nerves	Minimize maximum dose	5
Optic chiasm	Minimize maximum dose	5
Lenses	Minimize mean dose	5
Hippocampi	Minimize mean dose	3
Temporal lobes	Minimize mean dose	2
Cochleae	Minimize mean dose	1
Brain excluding other ROIs	Minimize mean dose	1

VMAT trajectory used a single gantry arc from 179° to 181°, with maximum couch and gantry rotations between adjacent control points of 2°. No additional processing or smoothing was performed on the trajectories prior to treatment planning or delivery. Couch rotation speed between adjacent control points was not explicitly included in treatment plan optimization but was determined by the linac control system at delivery.

As dynamic couch motion during beam delivery was not supported within the clinical TrueBeam control software, plans were delivered using research and development access with motion restrictions removed ("Developer Mode"). AutoBeam DICOM plan files were converted to Extensible Mark-up Language (XML) format for Developer Mode delivery (Varian Medical Systems 2013) using Veritas v2.2 (Mishra *et al* 2014). The steps from trajectory optimization to plan delivery, comparisons performed, and systems used are summarized in Figure 1.

2.3. Dosimetric accuracy

A 30 cm x 30 cm x 30 cm phantom, consisting of multiple slabs of solid water, was used for dosimetric verification. The expected dose distribution for each treatment plan when delivered to the verification phantom was calculated in Pinnacle^3. The Adaptive Convolve algorithm and a 2.0 mm x 2.0 mm x 2.0 mm resolution dose grid were used for all cases.

For each plan, a position for point dose measurement was identified in a region of homogeneous dose within the PTV. A region of interest (ROI) that approximated the 0.125 cm^3 collecting volume of a Semiflex ionisation chamber (PTW, Freiburg, Germany) was contoured, centred on the measurement position, and the mean dose to the ROI for a single fraction delivery defined the predicted dose. Measurements were performed using the Semiflex chamber and a Unidos electrometer (PTW, Freiburg, Germany); three measurements were taken and averaged for each plan.

Radiochromic film measurements were performed using EBT3 (Lot number

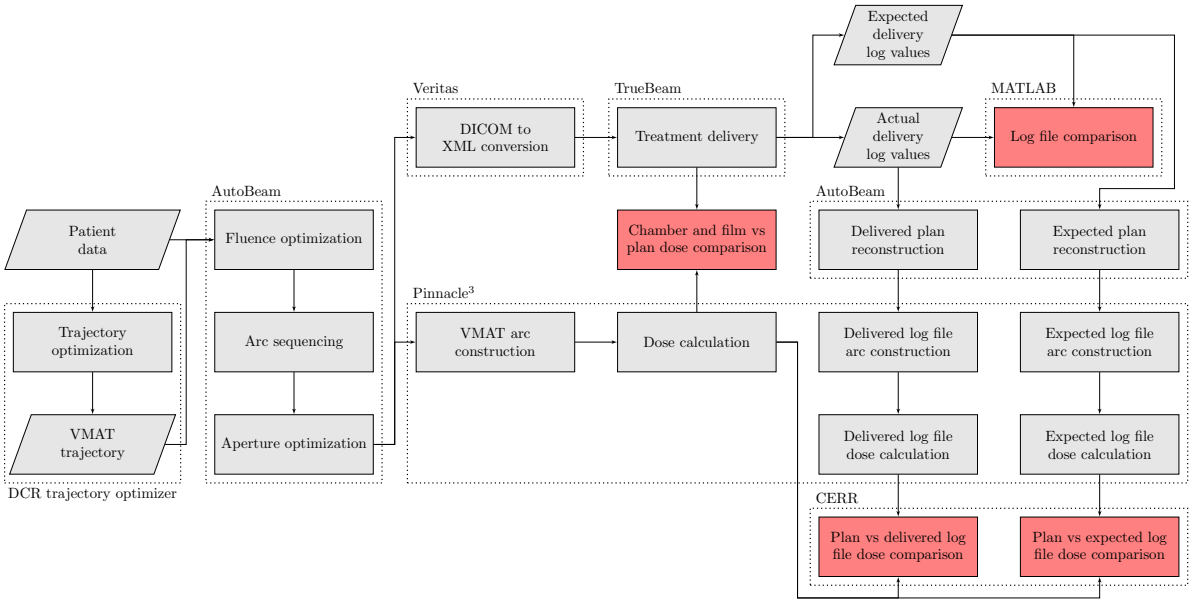

Figure 1. Flowchart showing the steps from plan generation to delivery (light boxes) and the comparisons investigated in this paper (dark boxes). Dashed boxes indicate the software or hardware in which the steps were performed.

04051602; Ashland Advanced Materials, Bridgewater, NJ). To characterize the dose to colour value conversion for the film batch, six strips were cut from a single sheet of film and irradiated to 25, 50, 100, 200, 400 and 800 cGy in a water-equivalent phantom, in line with Lewis and Chan (2015) and manufacturer recommendations‡. A seventh film strip was left unirradiated. Films were scanned using an Epson 11000XL flatbed scanner (Epson America, Inc., Long Beach, CA) in transmission mode, with a resolution of 72 dpi. To reduce uncertainties caused by film curling, a 2 mm thick glass compression plate was placed on top of the films during scanning (Palmer *et al* 2015). Films were analysed using FilmQA Pro (v3.0, Ashland Advanced Materials, Bridgewater, NJ) software.

Coronal and sagittal planes through the PTV were measured for each VMAT and DCR-VMAT plan. Two film strips were cut from each film sheet, one of which was irradiated to 170 cGy, and used to scale the calibration curve for that measurement (Lewis *et al* 2012). Dosimetry was analysed using the triple channel method to mitigate uncertainties due to the film scanner and variations in film thickness (Micke *et al* 2011). Film to plan registration was performed by aligning the marked film isocentre position with the plan isocentre position, small discrepancies between marked and actual film position were removed using the optimization option in FilmQA Pro. Comparison of red colour channel measurements with predictions was performed using two-dimensional gamma analysis with criteria of 3% (global dose difference normalisation) and 3 mm ($\gamma_{3G/3}$). Analysis with a stricter distance to agreement criterion of 1 mm ($\gamma_{3G/1}$) was also performed. When reporting passing rates for gamma analysis, pixels below a low

‡ Efficient Protocols for Accurate Radiochromic Film Calibration and Dosimetry http://www.gafchromic.com/documents/Efficient%20Protocols%20for%20Calibration%20and%20Dosimetry.pdf

dose threshold of 20% were excluded (Clark *et al* 2014).

2.4. Linac log file analysis

Linac log files were acquired during delivery of each treatment plan. TrueBeam log files record the primary readout of the linac motion axes and MLC leaf positions every 20 ms during beam delivery, as well as values interpolated from the original DICOM plan (Eckhause *et al* 2015). These form "delivered" and "expected" log file values, respectively, making it possible to determine mechanical errors every 20 ms during treatment. Expected and delivered log file values for gantry rotation, couch rotation, and all MLC leaves were extracted using a MATLAB (v2010b, The Mathworks, Nantick, MA) script. For each parameter the root-mean-square error (RMSE) was calculated according to Equation 1.

$$RMSE = \sqrt{\frac{1}{N}\sum_{1}^{N}(D_n - E_n)^2} \tag{1}$$

where N was the total number of log file samples, and D and E were the delivered and expected log file parameter values for sample n.

To determine if RMSE values of individual MLC leaves were correlated with the total motion of the MLC leaf, Spearman's rank correlation coefficients were calculated in MATLAB. This was performed for each MLC leaf bank for both VMAT and DCR-VMAT. If the p-value associated with a correlation coefficient was less than 0.05, the correlation was judged to be statistically significant.

2.5. Linac log file dose reconstruction

The dosimetric difference between the Pinnacle^3 treatment plan and dynamic plan delivery was determined by reconstructing a plan from each log file. VMAT and DCR-VMAT plans were created in Pinnacle^3 with control points specified by the delivered log file values of gantry rotation, couch rotation, aperture shape, and cumulative monitor units. To reduce the control points to a manageable number for calculation within Pinnacle^3, every fifth log file sample was used, resulting in a beam with ten control points per second. Reconstructed plan doses were calculated on the patient CT data using the local clinical standard settings of a 2.5 mm x 2.5 mm x 2.5 mm dose grid resolution and the Adaptive Convolve algorithm.

Planned and delivered dose cubes were exported to CERR v5.2 (Deasy *et al* 2003) for comparison using three-dimensional (3D) gamma analysis for all voxels above a 5% low dose threshold with 2% and 2 mm acceptance criteria ($\gamma_{2G/2}$). Dose criteria were relative to the global maximum of the planned dose cube, which was used as the reference distribution. Both dose calculations shared the same beam model, dose grid settings, and dose calculation algorithm. This left two sources of error in this comparison: (1) the number of control points used to calculate the dose, and (2) the mechanical errors recorded in the delivered log file. Therefore, stricter gamma analysis criteria were used

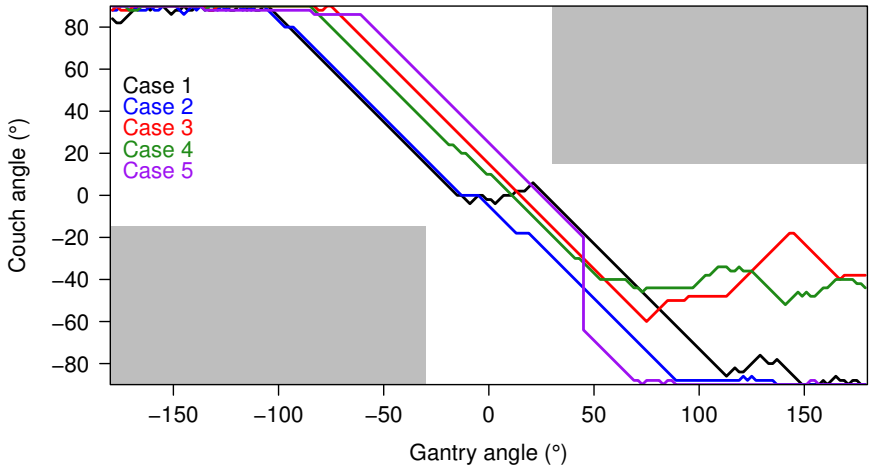

Figure 2. DCR-VMAT trajectories optimized for each patient case. The shaded corner regions indicate forbidden areas of the solution space where collisions between the linac gantry and patient or patient couch were likely.

for these comparisons than for the radiochromic film measurements. To identify the main cause of any discrepancies, an additional dose distribution was reconstructed from the expected linac log files and compared with the original treatment plan.

3. Results

3.1. Beam modelling

Absolute point dose measurements and relative output factors of jaw-defined fields used for TrueBeam model validation were within ±1% of predictions. Pinnacle[3] percentage depth doses and profiles agreed with validation measurements to within 2% or 2 mm (generally 1% or 1 mm). Results for the validation of modulated delivery using coplanar VMAT plans are presented in Section 3.3 to allow direct comparison against DCR-VMAT measurements.

3.2. Treatment planning and delivery

Optimized DCR-VMAT trajectories are shown in Figure 2. Axial, coronal, and sagittal views of DCR-VMAT treatment plans for each case are shown in Figure 3. Dose volume histograms for VMAT and DCR-VMAT plans are shown in Figure 4. Due to the relatively small number of cases investigated, results are quoted as median (range) values throughout. Monitor units were 276.3 (258.5–296.4) for DCR-VMAT compared with 239.9 (220.9–272.7) for coplanar VMAT. Delivery times were 125 s (123–133 s) for DCR-VMAT compared with 78 s (64–130 s) for coplanar VMAT. Monitor units, delivery times, and numbers of control points are presented for all cases in Table 3.

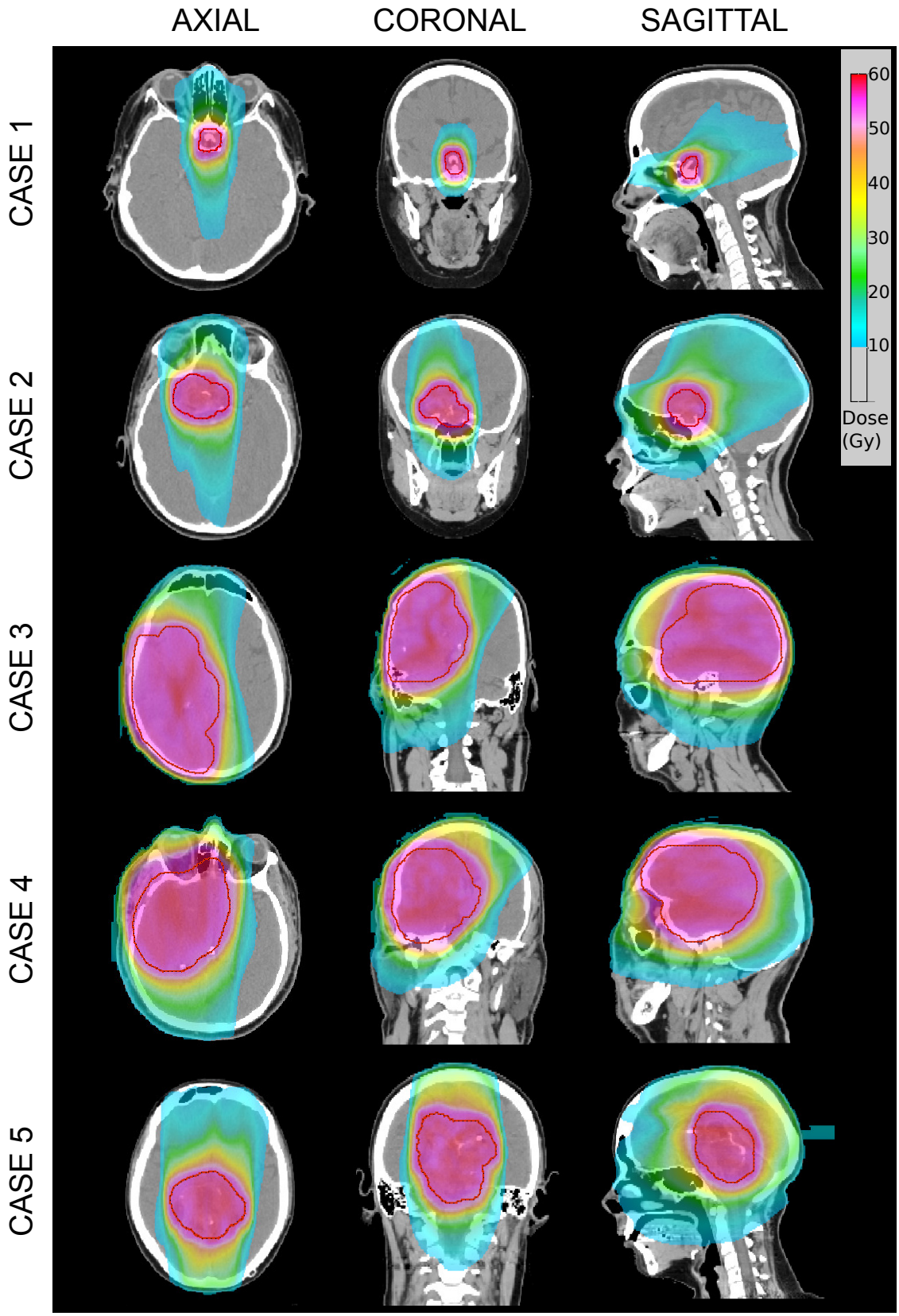

Figure 3. DCR-VMAT plan dose distributions presented on axial, coronal and sagittal views for all cases. The planning target volume (PTV) contour is overlaid on the dose colourwash.

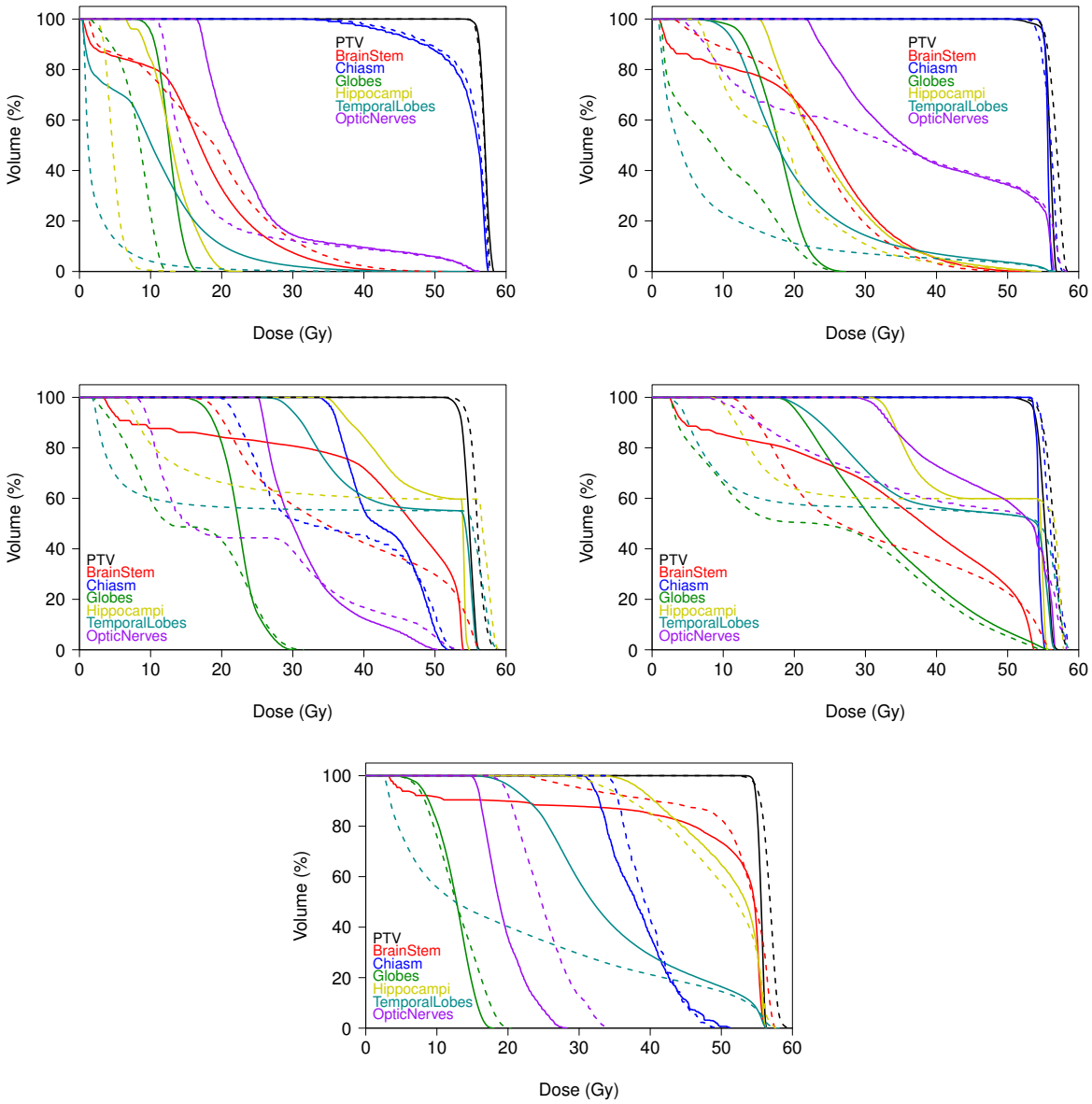

Figure 4. Dose volume histograms for each case, showing coplanar VMAT (solid line) and DCR-VMAT (dashed line) results.

Table 3. Monitor units, delivery times, and numbers of control points for VMAT and DCR-VMAT plans for each case.

	Monitor units		Delivery time (s)		Control points	
Case	VMAT	DCR-VMAT	VMAT	DCR-VMAT	VMAT	DCR-VMAT
1	272.7	296.4	64	133	180	180
2	251.5	283.5	65	128	180	180
3	220.9	258.5	126	123	180	180
4	229.2	262.6	130	123	180	180
5	239.9	276.3	78	125	180	202

Table 4. Predicted and measured absolute point doses for coplanar VMAT and DCR-VMAT plans.

	VMAT			DCR-VMAT		
	Dose (cGy)		Difference	Dose (cGy)		Difference
Case	Predicted	Measured	(%)	Predicted	Measured	(%)
1	135.2	136.0	0.6	140.7	141.5	0.6
2	133.4	134.6	0.9	137.0	139.3	1.7
3	134.7	136.5	1.3	136.4	137.2	0.6
4	138.9	140.9	1.5	133.8	134.9	0.8
5	135.2	137.3	1.6	142.3	143.5	0.8

Table 5. Percentage of coronal and sagittal film pixels receiving a dose of at least 20% with a gamma <1 at 3% / 3 mm and 3% / 1 mm for coplanar VMAT and DCR-VMAT plans.

	3% / 3 mm				3% / 1 mm			
	VMAT		DCR-VMAT		VMAT		DCR-VMAT	
Case	Coronal	Sagittal	Coronal	Sagittal	Coronal	Sagittal	Coronal	Sagittal
1	100	81.0	99.2	96.0	91.4	42.9	83.5	90.8
2	97.6	87.0	98.3	98.2	75.9	68.0	80.5	81.0
3	100	99.0	100	92.9	99.0	81.3	99.5	82.1
4	100	99.1	99.8	99.0	99.5	90.3	95.7	89.5
5	99.5	96.6	96.7	98.1	93.2	80.8	85.4	86.6

3.3. Dosimetric accuracy

Median (range) differences in absolute dose from plan prediction were 0.8% (0.6–1.7%) for DCR-VMAT compared with 1.3% (0.6–1.6%) for VMAT. Complete results are presented in Table 4. Linac output on the day of measurement, which remained as a potential source of uncertainty in the point dose results, was 0.4% higher than ideal.

DCR-VMAT median gamma analysis pass rates, for doses greater than a 20% threshold using $\gamma_{3G/3}$, were 99.2% (range 96.7–100%) for coronal and 98.1% (92.9–99.0%) for sagittal measurements. Coplanar VMAT gamma analysis pass rates were 100% (97.6–100%) for coronal and 96.6% (81.0–99.1%) for sagittal measurements. Analysis using gamma criteria of 3% and 1 mm ($\gamma_{3G/1}$) gave results of 85.4% (80.5–99.5%) for coronal DCR-VMAT, 86.6% (81.0–90.8%) for sagittal DCR-VMAT, 93.2% (75.9–99.5%) for coronal VMAT, and 80.8% (42.9–90.3%) for sagittal VMAT. Complete results are presented in Table 5. Further analysis of sagittal VMAT cases 1 and 2 using gamma criteria of 5% and 3 mm ($\gamma_{5G/3}$) gave results of 99.4% and 97.2%, respectively. Gamma analysis maps ($\gamma_{3G/3}$) and isodose comparisons for all DCR-VMAT cases are shown in Figure 5. Dose profiles for all DCR-VMAT cases are presented in Figure 6.

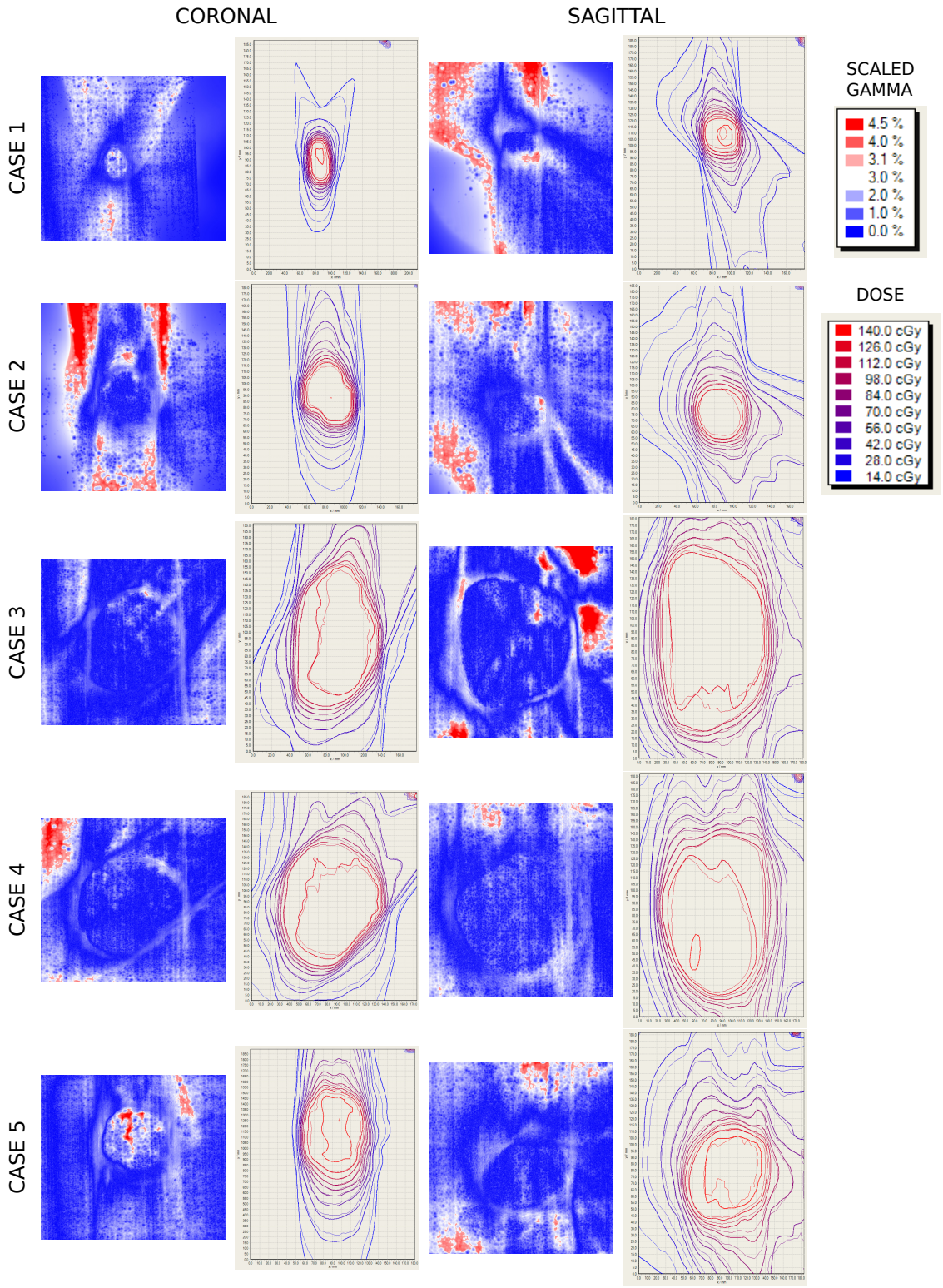

Figure 5. DCR-VMAT coronal and sagittal radiochromic film results for all cases. Gamma analysis results using 3% and 3 mm criteria with no dose threshold are shown for each measurement orientation. FilmQA Pro results are displayed as a product of the gamma result and the dose deviation criterion, meaning 3% represents a γ value of 1. Isodose comparisons are shown for each measurement orientation, with thick lines indicating the planned isodoses.

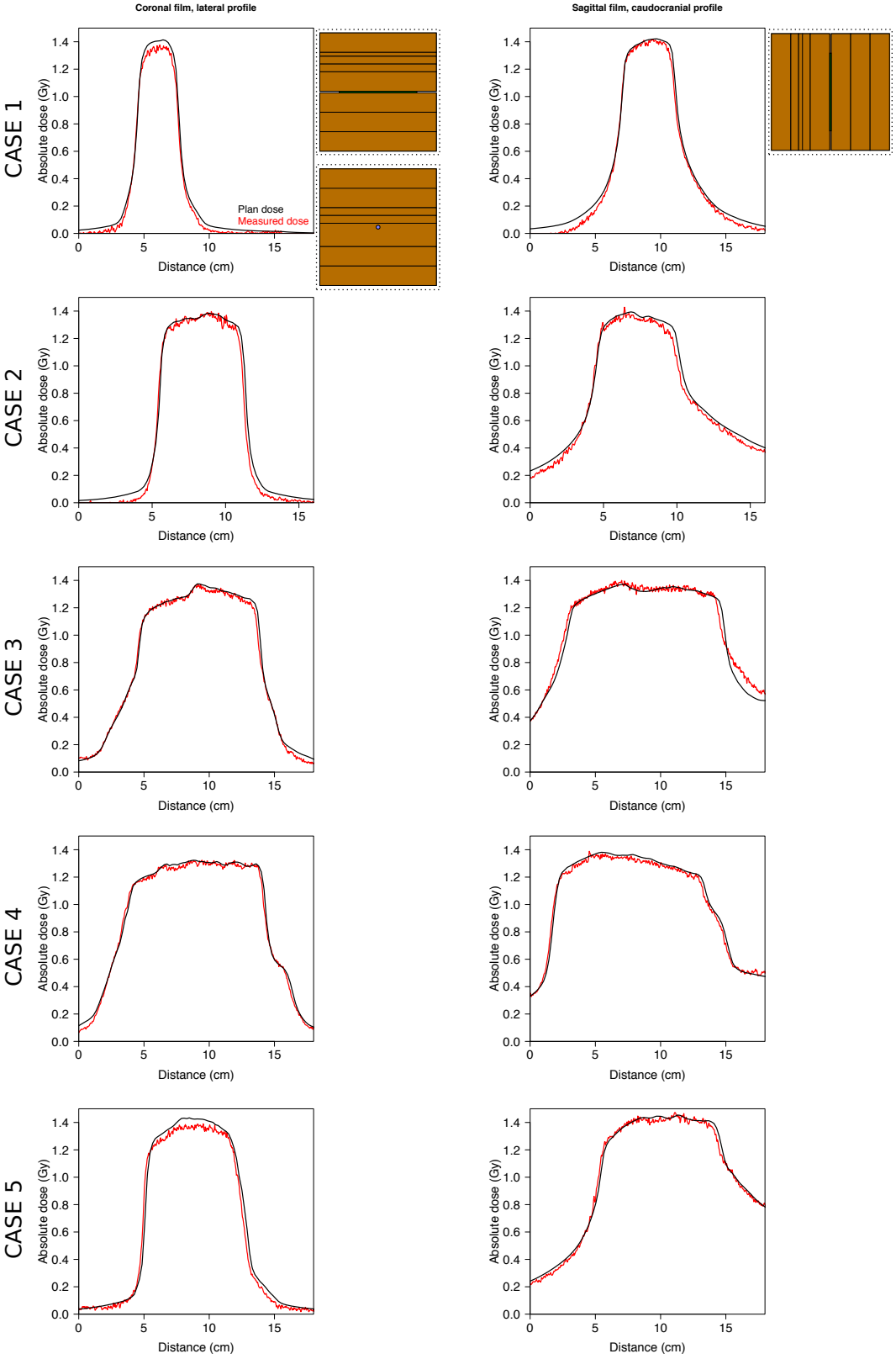

Figure 6. DCR-VMAT dose profiles for the sagittal and coronal film measurements for all cases. Phantom orientations are shown for coronal film, point dose chamber, and sagittal film measurements.

Table 6. Root-mean-square error of gantry rotation for VMAT and DCR-VMAT and couch rotation for DCR-VMAT.

	Gantry rotation (°)		Couch rotation (°)
Case	VMAT	DCR-VMAT	DCR-VMAT
1	0.051	0.059	0.102
2	0.057	0.056	0.091
3	0.055	0.057	0.094
4	0.054	0.058	0.086
5	0.067	0.051	0.086

3.4. Linac log file analysis

Linac log file analysis showed similar gantry rotation RMSE for coplanar VMAT (median 0.055°, range 0.051–0.067°) and DCR-VMAT (median 0.057°, range 0.051–0.059°). Couch rotation RMSE for DCR-VMAT was 0.091° (0.086–0.102°). Full results are presented in Table 6. Maximum couch rotation error for all VMAT cases was 0.002°. RMSE for individual MLC leaves are presented in Figure 7. Although all MLC errors were small, statistically significant ($p< 0.001$) strong correlations were found between RMSE and the total recorded leaf motion calculated from delivered log files. Spearman coefficients were 0.82 and 0.88 for coplanar VMAT (leaf banks A and B, respectively) and 0.83 for DCR-VMAT (both leaf banks).

3.5. Linac log file dose reconstruction

DCR-VMAT log file dose reconstructions produced plans with a median of 1239 (range 1210–1314) records, compared with 180 (180–202) control points used during treatment planning. For VMAT, log file dose reconstructions used 759 (626–1291) records compared with 180 control points during treatment planning.

Gamma analysis maps comparing DCR-VMAT treatment plan dose and reconstructed dose from delivered log files are shown in Figure 8. These evaluate the effect of errors due to the different number of control points used to calculate the dose and mechanical errors recorded in the log file. All comparisons reported 100% of voxels within the body ROI passing a $\gamma_{2G/2}$, however some case-specific differences were seen in the gamma analysis maps. The expected dose reconstructions, which excluded the effect of log file reported delivery errors, also reported 100% of voxels passing $\gamma_{2G/2}$ when compared to the plan dose. Absolute dose differences between delivered and expected dose reconstructions were within 0.3 Gy for all cases.

As the version of CERR used could not perform gamma analysis with local dose difference normalisation, or with distance criteria below half the voxel size, reanalysis with stricter gamma criteria (e.g. $\gamma_{2L/2}$ or $\gamma_{1G/1}$) was not performed. However, analysis using $\gamma_{2G/2}$ criteria was sufficient to identify any significant differences resulting from the finer positional sampling of the log file dose reconstructions for the clinical standard

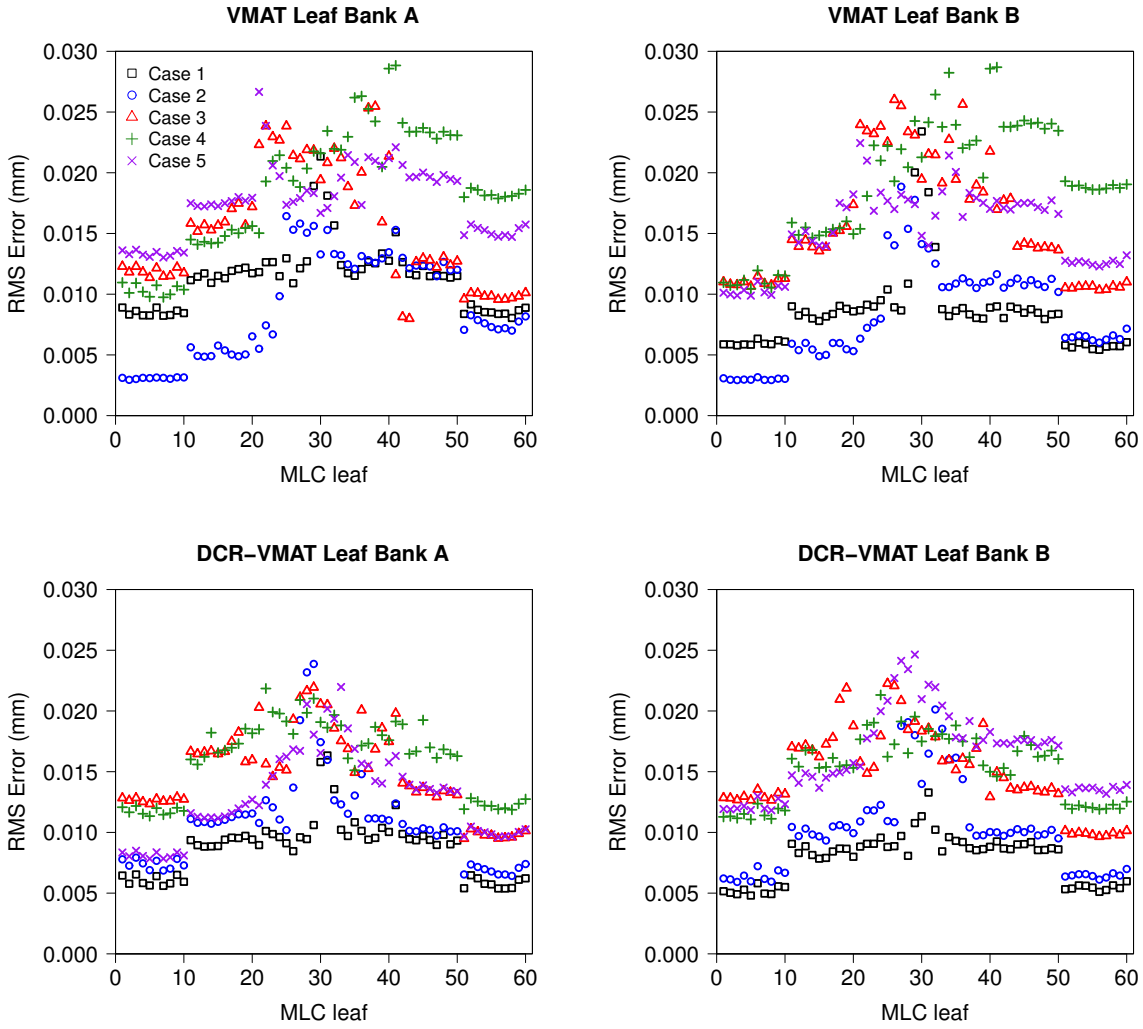

Figure 7. MLC root-mean-square errors for coplanar VMAT plans and DCR-VMAT plans for all Cases for MLC leaf banks A and B (left and right, respectively). MLC leaf banks A and B correspond to X2 and X1 in IEC 61217.

dose calculation resolution used.

4. Discussion

This paper describes the dosimetric accuracy of single arc DCR-VMAT for five primary brain tumour cases. DCR-VMAT meets clinical standards of dosimetric accuracy, with point dose measurements all within 2% and gamma analysis ($\gamma_{3G/3}$) pass rates >90% (most >95%) for coronal and sagittal radiochromic film measurements. There are several possible sources of uncertainty in the point dose and film measurements, including any discrepancies between the delineated chamber volume and the effective measurement point in the phantom, any deviation of the actual solid water block densities from the water density assigned in the TPS, errors in phantom positioning and alignment,

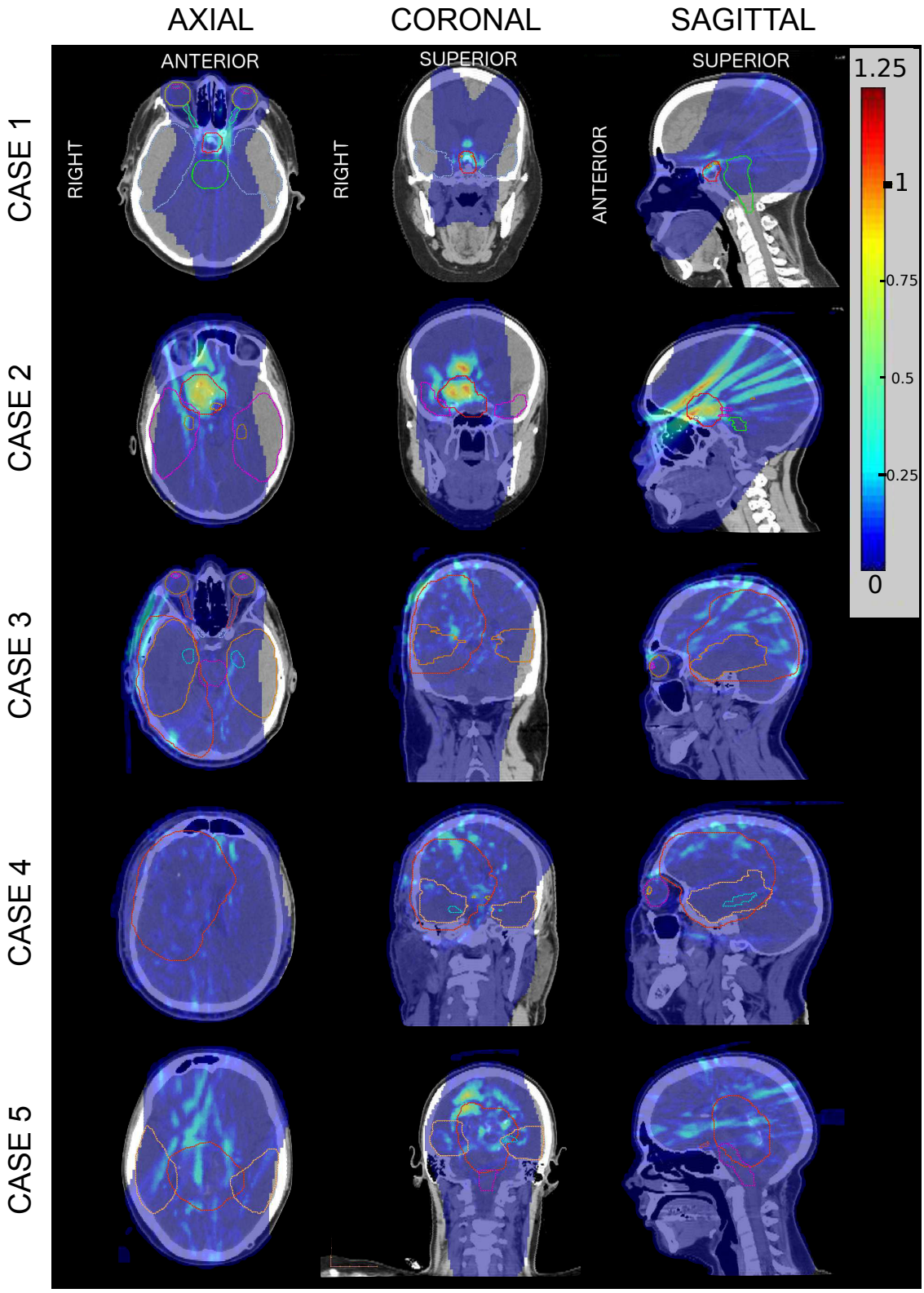

Figure 8. Gamma analysis results, comparing the treatment plan dose distribution against the dose distribution reconstructed from delivered log file parameters. Axial, coronal and sagittal views are presented for all cases. Gamma analysis used acceptance criteria of 2% and 2 mm for doses above a 5% threshold. Red colour wash indicates $\gamma > 1$.

and uncertainties in the film calibration or readout. We have attempted to minimize these uncertainties in practice. However, Vera-Sánchez *et al* (2018) have calculated the uncertainty in absolute dose measurement for triple-channel film dosimetry using Epson 10000XL flatbed scanners to be 2–3% for the target doses measured in this study. For doses close to the low dose threshold used in our analysis, they calculate that the uncertainty increases to 10%.

The scope of this study is limited to conventionally fractionated primary brain tumours to evaluate the feasibility of DCR-VMAT treatment delivery for a site where it has demonstrated potential clinical benefit (Smyth *et al* 2016). Although primary brain tumours may not require the extensive MLC modulation necessary for sites such as the head and neck (Fix *et al* 2018), more complex trajectories can be used due to the larger non-collisional space around the patient (Wilson *et al* 2017). Further investigation of the plan quality and dosimetric accuracy for other sites that may benefit from DCR-VMAT, including stereotactic indications in the brain and body, is warranted in a future study.

A full dosimetric comparison of the two techniques used in this paper has been presented in Smyth *et al* (2016) for a 15-patient cohort of primary brain tumours. Relevant dose volume histogram parameters for PTV and OARs, integral dose, conformity, homogeneity, and gradient indices are presented and analysed. DCR-VMAT is shown to produce statistically significant differences in PTV homogeneity that are judged to be clinically acceptable in light of significant OAR sparing over VMAT. The cases presented here are a subset of that cohort and the plans produced differ from Smyth *et al* (2016) only in the linac model used (TrueBeam vs Synergy (Elekta AB, Stockholm, Sweden) with Agility MLC) and the method of target dose normalisation in Pinnacle^3 (not normalised vs normalised to PTV mean dose). In this work, vertex segments of arc are permitted during trajectory optimization, which could result in an undesirable volume of very low exit dose through the patient's length. While some of this low dose can be constrained during plan optimization, an alternative approach is to explicitly exclude from trajectory optimization any beam orientations where the beam would continue through the patient beyond the limits of their CT scan (Wild *et al* 2015).

These results are consistent with the data presented in the literature to date for other techniques using dynamic couch rotation. Fahimian *et al* (2013) report a single TMAT delivery for a prone partial breast treatment plan. The deviation of point dose measurement from plan prediction is 2.4%, while the gamma analysis pass rate for $\gamma_{3G/3}$ is 93%. In a follow-up paper, Liang *et al* (2015) also report results for a single delivery. For that case, the deviation in measured point dose from plan prediction is 1.6% and the gamma analysis pass rate for $\gamma_{3G/3}$ is 90.2%. Wilson *et al* (2017) report the validation of TVMAT is within 2.2%, and 96–100% of film pixels meet gamma criteria of $\gamma_{2G/2}$ for the four plans under investigation. Manser *et al* (2018) investigate the dosimetric accuracy of a manually defined DCR-VMAT trajectory for a prostate case and find 96% of diodes meet gamma criteria of $\gamma_{2G/2}$ in comparison to a research Monte Carlo dose calculation. Fix *et al* (2018) report 99.5% of radiochromic film pixels meet gamma

criteria of $\gamma_{2G/2}$ for a head and neck DCR-VMAT treatment plan that uses geometric trajectory optimization and a Monte Carlo dose calculation. The results in our paper use a commercial adaptive convolution superposition dose calculation algorithm and are consistent with reports of coplanar VMAT in a national audit using a diode array (Clark *et al* 2014). The median (range) passing rate for $\gamma_{3G/3}$ is 98.8% (83.8–100%) for linac and TPS combinations that do not share a common vendor (Type 2 combinations), as is the case in this work.

Passing rates for $\gamma_{3G/3}$ may be insensitive to clinically significant errors introduced during treatment planning or TPS commissioning, particularly when using arrays, but these risks can be mitigated by evaluating deviations in point doses and dose profiles (Nelms *et al* 2013) as performed in our paper. Gamma analysis results can also vary significantly between measurement devices and calculation software (Hussein *et al* 2017). Future work on DCR-VMAT should include a systematic investigation of gamma analysis sensitivity to technique-specific error combinations (e.g. miscalibration of machine parameters, such as couch rotation and MLC position, or patient misalignment) for a range of clinical sites using multiple measurement devices.

A limitation of the measurements in this paper is that they do not use an anthropomorphic phantom. However, other groups also report results in water equivalent plastic (Fahimian *et al* 2013, Liang *et al* 2015, Wilson *et al* 2017, Fix *et al* 2018). Using a cubic phantom, as in our study, may increase the chance of detecting errors that have been caused by inaccurate MLC, gantry, and couch synchronization, when compared to an anthropomorphic head phantom with more gradual changes in contour. Another limitation is that the measurements in this work only measure planar dose distributions. Although it is common to use detector arrays that may also interpolate between multiple measurement planes and evaluate the full three-dimensional dose distribution, the use of these devices generally requires a coplanar delivery. Verification of DCR-VMAT plans must also include the contribution of the dynamic couch motion, which rules out the use of gantry-mounted diode arrays. Alternative volumetric measurement techniques, such as gel dosimetry, should be explored in future work.

Log file reported errors that have been determined for DCR-VMAT are small and have limited dosimetric effect. Wilson *et al* (2017) analyse log files for TVMAT deliveries and report couch rotation RMSE of 0.041–0.051° and gantry rotation RMSE of 0.042–0.050°. The larger couch rotation error results in this paper could be due to differences in inertia between the TVMAT and DCR-VMAT techniques. TVMAT rotates the couch fully in one direction before sweeping back, while the optimized DCR-VMAT trajectories that have been investigated in this paper allow either clockwise or anti-clockwise rotations throughout (Figure 2). In a previous study, a simulated systematic 2° error in couch rotation for DCR-VMAT increases OAR dose by up to 10% (Smyth *et al* 2013), although a misalignment of that size is unlikely based on log file analysis. This work investigates log file reported errors, however Agnew *et al* (2014) and Neal *et al* (2016) demonstrate that there can be discrepancies between the log file reported and

physical positions of linac components that are not identified by log file analysis. Wilson and Gete (2017) recommend validating the accuracy of log file records and suggest techniques for couch rotation. Although not performed in our study, this validation step would be crucial before using log file values for pre-treatment delivery quality assurance in the absence of dosimetric measurements such as those presented here.

This paper is the first to report linac log file dose reconstruction for dynamic couch rotation techniques. The large number of samples that has been used in reconstruction gives a close approximation of dynamic dose calculation and demonstrates that couch and gantry control point spacing of 2° models dynamic delivery on the treatment machine to within 2% and 2 mm. The dosimetric effect of linac reported mechanical errors, determined from the difference between delivered log file and expected log file dose reconstructions, was within 0.3 Gy for all cases in this study. Similar investigations for coplanar VMAT using Monte Carlo dose calculation find differences of approximately 2%, which is consistent with the results in this paper (Teke *et al* 2010, Boylan *et al* 2013). An alternative to static approximation during dose calculation is to model dynamic linac motion directly within Monte Carlo dose calculation (Manser *et al* 2018, Fix *et al* 2018), although this is not yet commercially available. Future work should investigate the validity of dose calculation for larger control point spacing.

DCR-VMAT delivery is slower than VMAT, with median (range) delivery times of 125 s (123–133 s) and 78 s (64–130 s), respectively. These differences are unlikely to be clinically important, especially when considering other aspects of the patient treatment such as pre-treatment verification imaging. Comparison with published data is challenging due to the different techniques and dose prescriptions that have been evaluated (Fahimian *et al* 2013, Wild *et al* 2015, Liang *et al* 2015, Wilson *et al* 2017, Fix *et al* 2018). Wild *et al* (2015) estimate times based on machine constraints for three intracranial plans, with results from 3.9 min to 6.9 min depending on the complexity of the trajectory and patient geometry. Fix *et al* (2018) report an average increase in beam on time of 20% for DCR-VMAT when compared with VMAT for five cases across four different tumour sites. For the brain cases that have been investigated in our study, the median increase in delivery time is 60.3% but range from a 5.4% decrease to a 108% increase. However, in the worst case the absolute increase in delivery time of DCR-VMAT over the corresponding VMAT plan is 69 s.

As with other delivery techniques, rigorous quality control testing of DCR-VMAT with strict tolerances is necessary (Wilson and Gete 2017). As well as existing tests for VMAT, additional tests to confirm accurate synchronous motion of linac gantry, couch, and MLC are required. Proposed synchronicity tests for VMAT (Bedford *et al* 2015, Mans *et al* 2016) and TMAT (Yu *et al* 2014) rely on the linac's on-board imaging device and therefore may not be feasible for DCR-VMAT due to the risk of collisions during non-coplanar motion.

Although we have shown that DCR-VMAT can be delivered accurately for the five cases studied, issues such as patient safety and comfort must be investigated prior to clinical implementation. Rotating the patient during treatment could induce

intrafractional motion, which may be mitigated using improved patient immobilization. Dynamic couch motion and the potential for patient-gantry collisions could also affect patient compliance. Performing a "Day Zero" simulation of the treatment with the patient present may be a simple method of providing reassurance, assuming technological issues have been resolved. Patient stability during dynamic couch motion should be further investigated in future work.

5. Conclusion

Results from the five patient cases in this paper suggest that clinical implementation of dynamic couch rotation during VMAT is feasible for primary brain tumours, provided that issues around patient safety, motion, and compliance are resolved. DCR-VMAT plans have been delivered to within a clinically acceptable level of accuracy and with a maximum delivery time of around 2 minutes using a commercial linear accelerator. Future work should focus on investigating patient compliance and intrafractional motion, and move towards implementing DCR-VMAT for primary brain tumours within a clinical trial.

Acknowledgments

We thank Carole Meehan and Richard Trouncer for providing TrueBeam commissioning data and David Bernstein for providing MATLAB scripts to access linac log file parameters. This paper represents independent research funded by the National Institute for Health Research (NIHR) Biomedical Research Centre at The Royal Marsden NHS Foundation Trust and The Institute of Cancer Research. The views expressed are those of the authors and not necessarily those of the NHS, the NIHR or the Department of Health and Social Care. Research at The Institute of Cancer Research is also supported by Cancer Research UK under Program C33589/A19727.

Conflict of interest statement

JLB receives research funding from Accuray Inc outside this work.

References

Agnew A, Agnew C E, Grattan M W D, Hounsell A R and McGarry C K 2014 Monitoring daily MLC positional errors using linac log file files and EPID measurements for IMRT and VMAT deliveries. *Phys. Med. Biol.* **59** N49

Bedford J L 2009 Treatment planning for volumetric modulated arc therapy.*Med. Phys.* **36** 5128–5138

Bedford J L 2013 Sinogram analysis of aperture optimization by iterative least-squares in volumetric modulated arc therapy. *Phys. Med. Biol.* **58** 1235–1250

Bedford J L, Chajecka-Szczygielska H and Thomas M D R 2015 Quality control of VMAT synchronization using portal imaging. *J. Appl. Clin. Med. Phys.* **16** 284–297

Boylan C J, Aitkenhead A H, Rowbottom C G and Mackay R I 2013 Simulation of realistic linac motion improves the accuracy of a Monte Carlo based VMAT plan QA system. *Radiother. Oncol.* **109** 377–383

Chang Z, Wu Q, Adamson J, Ren L, Bowsher J, Yan H, Thomas A and Yin F-F 2012 Commissioning and dosimetric characteristics of TrueBeam system: composite data of three TrueBeam machines. *Med. Phys.* **39** 6981–7018

Clark C H, Hussein M, Tsang Y, Thomas R, Wilkinson D, Bass G *et al* 2014 A multi-institutional dosimetry audit of rotational intensity-modulated radiotherapy. *Radiother. Oncol.* **113** 272–278

Deasy J O, Blanco A I and Clark V H 2003 CERR: a computational environment for radiotherapy research. *Med. Phys.* **30** 979–985

Dong P, Liu H and Xing L 2018 Monte Carlo tree search-based non-coplanar trajectory design for station parameter optimized radiation therapy (SPORT). *Phys. Med. Biol.* **63** 135014

Eckhause T, Al-Hallaq H, Ritter T, DeMarco J, Farrey K, Pawlicki T *et al* 2015 Automating linear accelerator quality assurance. *Med. Phys.* **42** 6074–6083

Fahimian B, Yu V, Horst K, Xing L and Hristov D 2013 Trajectory modulated prone breast irradiation: A LINAC-based technique combining intensity modulated delivery and motion of the couch. *Radiother. Oncol.* **109** 475–481

Fix M K, Frei D, Volken W, Terribilini D, Mueller S, Elicin O, Hemmatazad H, Aebersold D M and Manser P 2018 Part 1: Optimization and evaluation of dynamic trajectory radiotherapy. *Med. Phys.* **45** 4201–4212

Glide-Hurst C, Bellon M, Foster R, Altunbas C, Speiser M, Altman M *et al* 2013 Commissioning of the Varian TrueBeam linear accelerator: A multi-institutional study. *Med. Phys.* **40** 031719

Hussein M, Clark C H and Nisbet 2017 Challenges in calculation of the gamma index in radiotherapy - Towards good practice. *Phys. Med.* **36** 1–11

International Commission on Radiation Units and Measurements (ICRU) 2010 ICRU report 83 prescribing, recording, and reporting photon-beam intensity-modulated radiation therapy (IMRT). *J. ICRU* **10**

Krayenbuehl J, Davis J B and Ciernik I F 2006 Dynamic intensity-modulated non-coplanar arc radiotherapy (INCA) for head and neck cancer. *Radiother. Oncol.* **81** 151–157

Langhans M, Unkelbach J, Bortfeld T and Craft D 2018 Optimizing highly noncoplanar VMAT trajectories: the NoVo method. *Phys. Med. Biol.* **63** 025023

Lewis D and Chan M F 2015 Correcting lateral response artifacts from flatbed scanners for radiochromic film dosimetry. *Med. Phys.* **42** 416–429

Lewis D, Micke A, Yu X and Chan M F 2012 An efficient protocol for radiochromic film dosimetry combining calibration and measurement in a single scan. *Med. Phys.* **39** 6339–6350

Liang J, Atwood T, von Eyben R, Fahimian B, Chin E, Horst K, Otto K and Hristov D 2015 Trajectory modulated arc therapy: A fully dynamic delivery with synchronized couch and gantry motion significantly improves dosimetric indices correlated with poor cosmesis in accelerated partial breast irradiation. *Int. J. Radiat. Oncol. Biol. Phys.* **92** 1148–1156

Lyu Q, Yu V Y, Ruan D, Neph R, O'Connor D and Sheng K 2018 A novel optimization framework for VMAT with dynamic gantry couch rotation. *Phys. Med. Biol.* **63** 125013

MacDonald R L and Thomas C G 2015 Dynamic trajectory-based couch motion for improvement of radiation therapy trajectories in cranial SRT. *Med. Phys.* **42** 2317

Mans A, Schuring D, Arends M P, Vugts C A J M, Wolthaus J W H, Lotz H T *et al* 2016 The NCS code of practice for the quality assurance and control for volumetric modulated arc therapy. *Phys. Med. Biol.* **61** 7221–7235

Manser P, Frauchiger D, Frei D, Volken W, Terribilini D and Fix M K 2018 Dose calculation of dynamic trajectory radiotherapy using Monte Carlo. *Z. Med. Phys. in press, https://doi.org/10.1016/j.zemedi.2018.03.002*

Micke A, Lewis D F and Yu X 2011 Multichannel film dosimetry with nonuniformity correction. *Med. Phys.* **38** 2523–2534

Mishra P, Lewis J, Etmektzoglou T and Svatos M 2014 TH-C-12A-12: Veritas: An open source tool to facilitate user interaction with TrueBeam Developer Mode. *Med. Phys.* **41** 563

Neal B, Ahmed M, Kathuria K, Watkins T, Wijesooriya K and Siebers J 2016 A clinically observed discrepancy between image-based and log-based MLC positions. *Med. Phys.* **43** 2933–2935

Nelms B E, Chan M F, Jarry G, Lemire M, Lowden J, Hampton C and Feygelman V 2013 Evaluating IMRT and VMAT dose accuracy: Practical examples of failure to detect systematic errors when applying a commonly used metric and action levels. *Med. Phys.* **40** 111722

Palmer A L, Bradley D A and Nisbet A 2015 Evaluation and mitigation of potential errors in radiochromic film dosimetry due to film curvature at scanning. *J. Appl. Clin. Med. Phys.* **16** 425–431

Papp D, Bortfeld T and Unkelbach J 2015 A modular approach to intensity-modulated arc therapy optimization with noncoplanar trajectories. *Phys. Med. Biol.* **60** 5179–5198

Pasler M, Kaas J, Perik T, Geuze J, Dreindl R, Kunzler T, Wittkamper F and Georg D 2015 Linking log files with dosimetric accuracy — A multi-institutional study on quality assurance of volumetric modulated arc therapy. *Radiother. Oncol.* **117** 407–411

Phillips Medical 2013 *Recommended Varian TrueBeam Physics Parameters*

Podgorsak E B, Olivier A, Pla M, Lefebvre P-Y and Hazel J 1988 Dynamic stereotactic radiosurgery. *Int. J. Radiat. Oncol. Biol. Phys.* **14** 115–126

Popescu C C, Beckham W A, Patenaude V V, Olivotto I A and Vlachaki M T 2013 Simultaneous couch and gantry dynamic arc rotation (CG-Darc) in the treatment of breast cancer with accelerated partial breast irradiation (APBI): a feasibility study. *J. Appl. Clin. Med. Phys.* **14** 161–175

Shaitelman S F, Kim L H, Yan D, Martinez A A, Vicini F A and Grills I S 2011 Continuous arc rotation of the couch therapy for the delivery of accelerated partial breast irradiation: a treatment planning analysis. *Int. J. Radiat. Oncol. Biol. Phys.* **80** 771–778

Smyth G, Bamber J C, Evans P M and Bedford J L 2013 Trajectory optimization for dynamic couch rotation during volumetric modulated arc radiotherapy *Phys. Med. Biol.* **58** 8163–8177

Smyth G, Evans P M, Bamber J C, Mandeville H C, Welsh L C, Saran F H and Bedford J L 2016 Non-coplanar trajectories to improve organ at risk sparing in volumetric modulated arc therapy for primary brain tumors. *Radiother. Oncol.* **121** 124–131

Smyth G, Evans P M, Bamber J C and Bedford J L 2019 Recent developments in non-coplanar radiotherapy. *Br. J. Radiol.* **92** 20180908

Teke T, Bergman A M, Kwa W, Gill B, Duzenli C and Popescu I A 2010 Monte Carlo based, patient-specific RapidArc QA using Linac log files. *Med. Phys.* **37** 116–123.

Varian Medical Systems 2013 *TrueBeam Developer Mode Version 2.0 User's Manual*

Vera-Sánchez J A, Ruiz-Morales C and González-López A 2018 Monte Carlo uncertainty analysis of dose estimates in radiochromic film dosimetry with single-channel and multichannel algorithms. *Phys. Med.* **47** 23–33

Wilson B, Otto K and Gete E 2017 A simple and robust trajectory-based stereotactic radiosurgery treatment. *Med. Phys.* **44** 240–248

Wilson B and Gete E 2017 Machine-specific quality assurance procedure for stereotactic treatments with dynamic couch rotations. *Med. Phys.* **44** 6529–6537

Wild E, Bangert M, Nill S and Oelfke U 2015 Noncoplanar VMAT for nasopharyngeal tumors: Plan quality versus treatment time. *Med. Phys.* **42** 2157

Yang Y, Zhang P, Happersett L, Xiong J, Yang J, Chan M and Hunt M 2011 Choreographing couch and collimator in volumetric modulated arc therapy. *Int. J. Radiat. Oncol. Biol. Phys.* **80** 1238–1247

Yu V Y, Fahimian B P, Xing L and Hristov D H 2014 Quality control procedures for dynamic treatment delivery techniques involving couch motion. *Med. Phys.* **41** 081712